Field Performance Testing of a Floating Tidal Energy Platform - Part 2: Load Performance

Penny Jeffcoate [*1], Nick Cresswell [*2]

[*]*Sustainable Marine Energy Ltd, Edinburgh, U.K.*

[1] penny.jeffcoate@sustainablemarine.com

[2] nick.cresswell@sustainablemarine.com

Abstract – **Sustainable Marine Energy have developed a floating surface platform that hosts four SCHOTTEL Hydro Instream Turbines, with a combined platform rated power of 280kW. The PLAT-I platform has been undergoing Sea Acceptance Tests (SATs) in Scotland to determine performance across the range of operational modes.**

A numerical method for the evaluation of platform position limits and simulation results for mooring line loads are found to match well with SAT results, providing confidence for future platform deployments.

The platform's loads and motions are found to be directly related to velocity and thus drag. Loads are strongly affected by mode of operation, with the platforms peak loadings and axial motion in the thrust-dominated operating regime. Maximum lateral motion occurs when in maintenance mode due to reduced side-damping.

The platform performed well, and as expected, during the SATs and is due to be redeployed for the second phase of testing in 2018.

***Keywords*—Tidal energy; Floating Platform; Mooring Loads; Platform Motions**

NOMENCLATURE

ADP	Acoustic Doppler Profiler
ECM	Electromagnetic Current Meter
GPS	Global Positioning System
HAT	Highest Astronomical Tide
IEC	International Electrotechnical Commission
LAT	Lowest Astronomical Tide
PLAT-I	PLATform for Inshore Energy
PLAT-O	PLATform for Offshore Energy
SAT	Sea Acceptance Trial
SDM	SIT Deployment Module
SIT	SCHOTTEL Hydro Instream Turbine
UTM	Universal Transverse Mercator

I. INTRODUCTION

Prior to commercial development and deployment tidal energy devices must conduct Sea Acceptance Trials (SATs) to determine whether they perform as expected. This is particularly important due to the wide variation in tidal sites and tidal energy technologies. Tidal developments have traditionally focused on highly energetic sites with extreme environmental conditions [1]. This is not restricted to high flow speed sites, but also sites with large wave conditions, for example at EMEC [1]. This results in either large surface platforms, such as Scotrenewables SR2000 [3], or subsurface platforms e.g. Sustainable Marine Energy's (SME) PLAT-O platform [4]. As focus in the industry moves away from UK waters towards other markets, such as South East Asia where sites have less extreme conditions, then new turbine and platform designs have been developed.

II. PLAT-I

SME have developed a surface variant of their platform to support third-party turbines, called PLAT-I. PLAT-I is a three-hulled tidal energy platform which hosts four SIT250s [4][5]. The turbines are suspended from the cross-deck, via lifting support structures called SIT Deployment Modules (SDMs). During generation or when parked, the turbines are in the down configuration, but they can be lifted clear of the water for operations and maintenance.

The platform self-aligns to incoming flow via a mooring turret which is connected to a geostationary mooring spread. During Sea Acceptance Trials of PLAT-I at Connel, Oban, Scotland the system was moored via a four-point spread and Raptor rock anchors [6]. The semi-catenary moorings are comprised of four chain sections, from the four anchor points, which are connected by tri-plates to fore and aft hawsers on the mooring turret (shown later in Figure 3).

III. SEA ACCEPTANCE TRIALS

Prior to commercial deployment PLAT-I was deployed in Connel, Oban for Sea Acceptance Trials. During this trial the platform was tested in various modes and operational states.

A. Connel, Oban

The test site used for the SATs is at Connel, Oban, at the mouth of Loch Etive, as shown in Figure 1. This is a sheltered sea loch with a large tidal zone, creating strong flows, but minimal wave conditions. The site is only exposed to the West, but surrounding coast and islands reduce the fetch and therefore the wave climate.

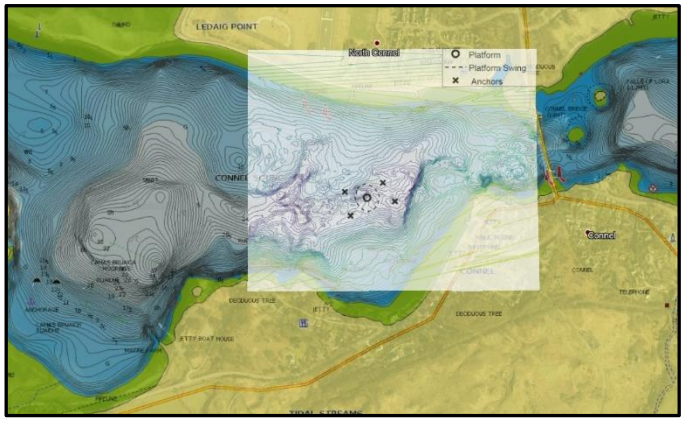

Figure 1: PLAT-I position at Connel, Oban

The site at Connel is ideal for trial deployments, as the flow speed on the ebb is driven by a jet formed by the Falls of Lora. This gives very localised fast flow, but with calm surrounding conditions for access and support infrastructure. Additionally, the flood tide has low flow velocities, giving long operational windows for maintenance.

The tidal jet on the ebb creates a strong localised flow but does result in high temporal and spatial variation in flow speed. This gives a very rigorous test environment for the multi-turbine platform.

Figure 2: PLAT-I operational during SATs at Connel, Oban

B. Instrumentation

Instruments were mounted on the platform to measure the water velocity, turbine performance, reaction force at the SDM (due to rotor thrust and SDM drag), mooring line load, and platform position. These are detailed in Table 1 and Figure 3, with the schematic of the platform and mooring system (turbine instrumentation detailed in Part 1). All instruments used for this part of the SATs recorded at 1Hz.

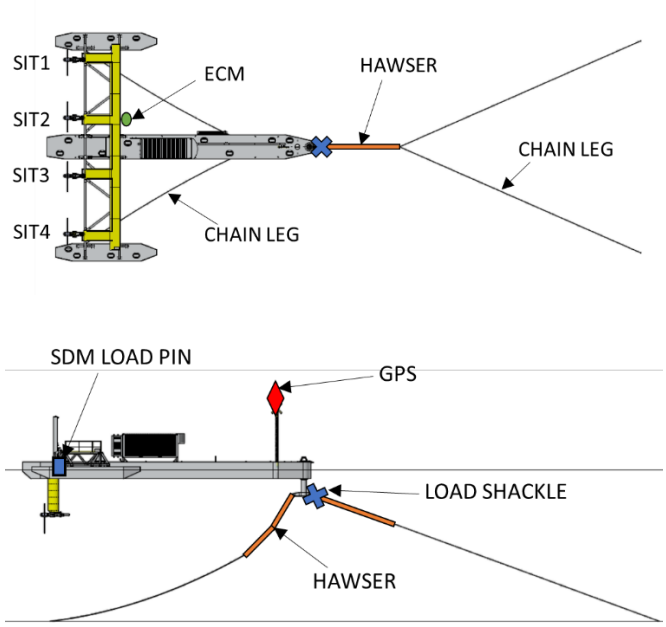

Figure 3: PLAT-I and Mooring System, with instrumentation locations

TABLE I
Test Instrumentation

Parameter	Instrument	Location
Velocity	Valeport Electromagnetic Current Meter	6.1m upstream from SIT2, 0.27m below water surface
Reaction force at pins	LCM Load Pin	Lower connection point between SDM and crossdeck structure
Mooring line load	Strainstall Mooring Shackle	Connection between mooring hawser and turret pad eye
Position	GPS	Top of mast

C. Tests

The platform was installed at the end of November 2017. The operational modes assessed during the SATs were SDMs up, SDMs only, SDMs down and rotors parked, or SDMs down and turbines operational (generating). These test modes are shown in Figure 4.

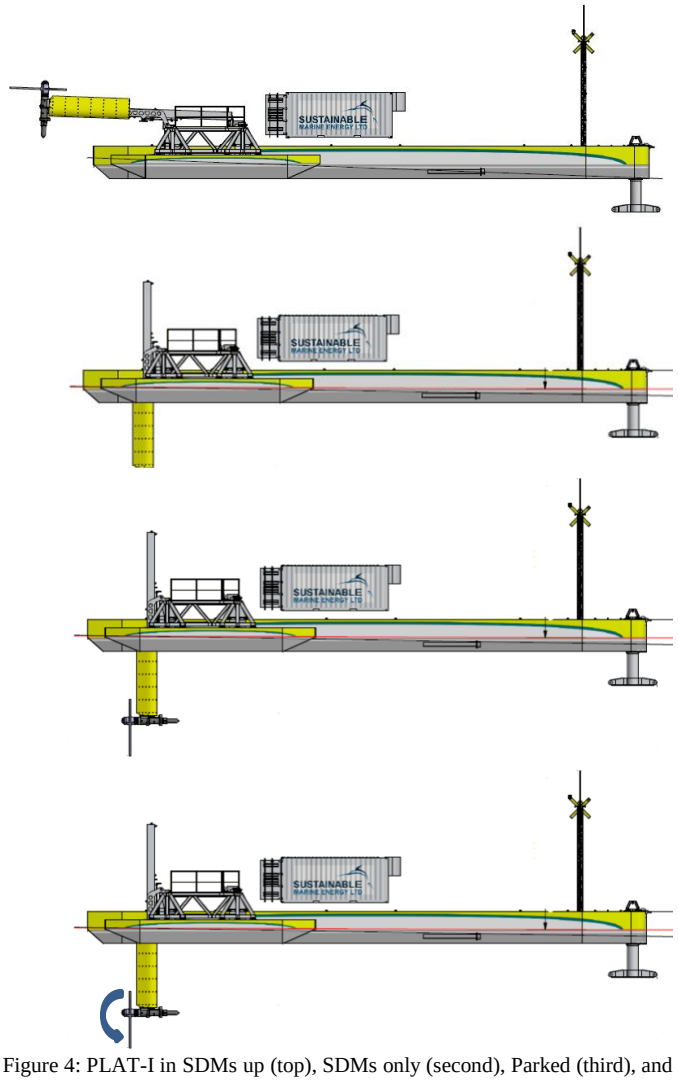

Figure 4: PLAT-I in SDMs up (top), SDMs only (second), Parked (third), and Operational (bottom) modes

Many different turbine and SDM configurations and operational parameters were assessed during the SATs. To assess mooring performance the platform requires all turbines to be in the same configuration. The test results presented will therefore use modes where are SDMs were up, all SDMs down (though not presented here), all turbines parked, and all turbines operating. The system was in each of these modes for several days of testing. Additionally, there were limitations to operating hours, and as such the turbines were only generating during daylight hours. Outside of this the rotors were parked.

For Part 2 the performance of the platform and mooring system will be investigated, including thrust and drag loads, and station keeping performance. The results from the GPS, ECM, SDM load pins, and mooring shackle will be used.

IV. Numerical Modelling of Position

The mooring centre and maximum departure of the platform have been assessed by finding the maximum and minimum axial and transverse departures. To find the axial turret departures the method detailed below is used:

1. Find ARC_{ij} (shown in Figure 5) at intersection of SP_i and SP_j, where the spheres are centred on anchor points and with radius equal to chain length.
2. Find plane on which ARC_{ij} sits.
3. Find coordinates of point P_{ij}, where point P_{CON} is on plane PL_{ijt}, P_{CON} is at connection depth and P_{ij} is on the plane described by ARC_{ij}.
4. Extract coordinates of point P_{CON}.

The transverse departure uses the method above, but the connection which is assessed is now the turret connection. Once excursion maxima and minima are known an ellipse can be fitted to the points to describe the locus for a given water depth.

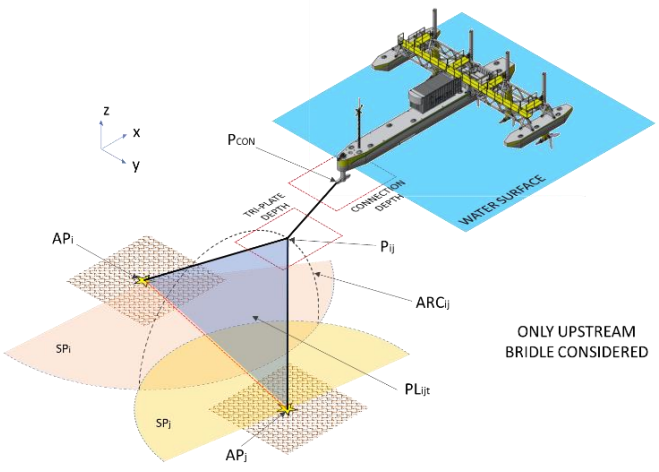

Figure 5: Assessment method for axial platform departure

V. Data Processing

Data was gathered from PLAT-I in the field and processed as described in Part 1 [7]. The position, velocity, SDM load and mooring loads are used for the following data analysis.

A. Position Data

In order to demonstrate the platform's positional stability, the GPS position of the mast was recorded. This is close to the turret head, so gives a good representation of the mooring excursion, without being significantly affected by the platform motion, though some yaw will cause greater motion. The raw 1Hz data was used to determine the motion of the platform due to the mooring excursion, in order to assess the full extent of the motion. The mast is 0.75m to Port and 1.7m aft of the turret head. As no platform orientation data was available at the time of writing, the GPS position was shifted using these offsets along the mean ebb flow vector, to determine the platform turret position. This inherently causes an offset in the opposite direction for the flood results, but since the system was not operating during this time then this was not considered.

This data is used concurrently with the 1Hz velocity measured by the ECM, which is located upstream from SIT2 on the Port side. This gives a representative velocity that the platform is experiencing, though there is some spatial variation in the flow. The positional stability with operational mode and velocity will be presented, using the GPS position.

B. Load Data

The SDM reaction load recorded at the bottom interface pin is also used here. This load is resolved to the force acting at the rotor nacelle, so is equivalent to a thrust force. The data used for this is IEC 2-minute averaged data, as discussed in Part 1 [7]. This removes variation due to the turbulence and spikes in the data. The variation in thrust between SITs and modes of operation will be presented.

The IEC 2-minute averaged mooring line load will also be presented, showing the variation in mooring load for different modes of operation.

The SDMs Up and Parked results are presented for both the ebb and flood tide but note that the ebb is significantly stronger (up to 4m/s instantaneous and 2.5m/s time-averaged, as opposed to less than 1m/s on the flood). The Operational results are presented for the ebb (West going) tide only, as this stronger flow results in the turbines reaching cut-in speed, through to rated power on spring tides. The mooring load shackle is installed on the East mooring hawser, so gives the upstream load when the platform is orientated to the ebb tide.

VI. Position

A. SDMs Up

The GPS position whilst the SDMs are raised, corrected to turret position, is shown in Figure 6 (red markers). This shows the 1Hz GPS position converted to UTM zone 30V. The calculated mooring centre (black circle), maximum turret departure at LAT and HAT (dashed line ellipses), and the mean ebb flow direction (dashed line at 249°) are also shown.

The platform position is clearly within the bounds estimated from the engineering predictions of mooring departure. The platform turret head is within approximately ±5m East/West, but there is significantly more motion North/South (±12m). There is high lateral motion, due to windage caused by a large wind profile area (as the SDMs are up), and low drogueing effect as the platform has a low draft. There is also little lateral

restraint from the mooring system as the restoring force from the catenaries is primarily in the flow direction.

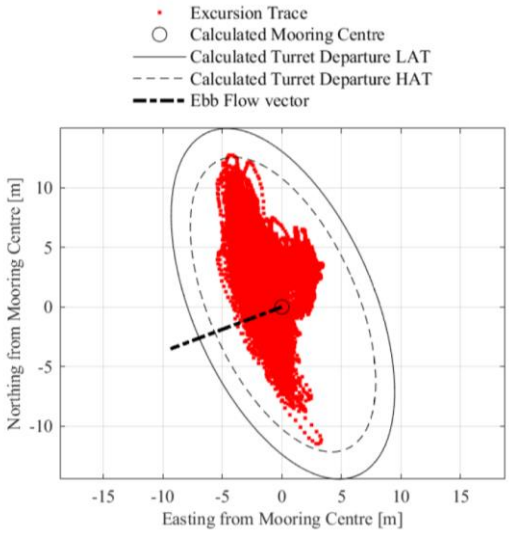

Figure 6: PLAT-I turret position with SDMs Up

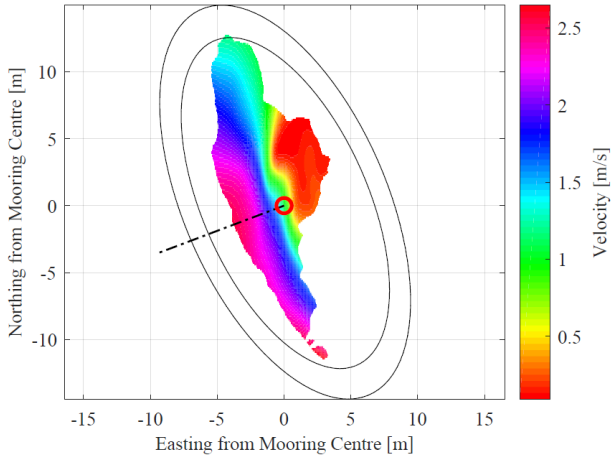

Figure 7: PLAT-I turret position with SDMs Up, with Velocity

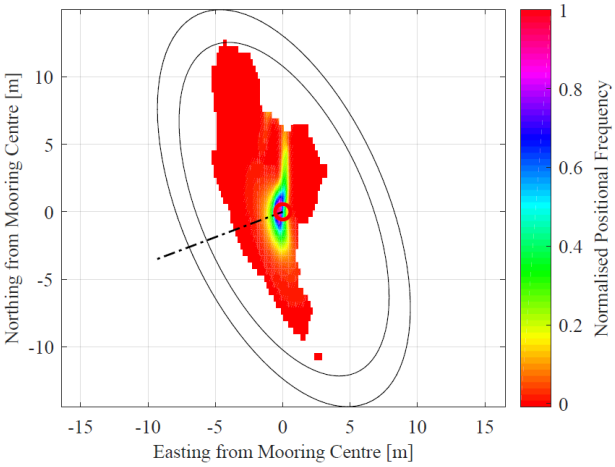

Figure 8: PLAT-I turret position with SDMs Up, with Occurrence

Large departures are particularly observed when the platform is to the West of the mooring centre, so aligned to the ebb tide, which is stronger and more turbulent. This motion, due to stronger flow, is seen by comparing position with velocity; Figure 7 shows the GPS position with a surface created using the mean velocity at each GPS position. This shows that the flood tide is weak (North East of the mooring centre) and so the platform sits close to the mooring centre (note that the offsets applied for the ebb results cause the flood position to be further north and East than actual platform position; this will be corrected in further analysis using platform orientation). The low load also allows a catenary effect in the upstream mooring lines, enhancing this position effect.

On the ebb, as the flow speed increases the platform moves to the West South West. The amount of lateral motion increases due to the turbulence and lack of resistance to side loading. The extreme southerly position in Figure 7 is the result of a single track as seen in Figure 6, likely due to the passing of a large eddy.

The positional stability can be seen in Figure 8, which shows the occurrence frequency of each position. This shows that for the vast majority of the time the system is close to the mooring centre, so the system is stable.

B. Parked

With the SDMs lowered and the turbines in Parked mode there are additional structures below the waterline, less above the waterline, and increased cross-sectional area perpendicular to the flow. The resulting excursion of the platform is shown in Figure 9 which shows that the North/South side motion has reduced, and the East/West motion has increased; this is due to increased draft and drag caused by the SDMs and rotors, increased dampening of side motion through SDM resistance, and to a certain extent reduced windage. The system is still well within predicted excursion limits.

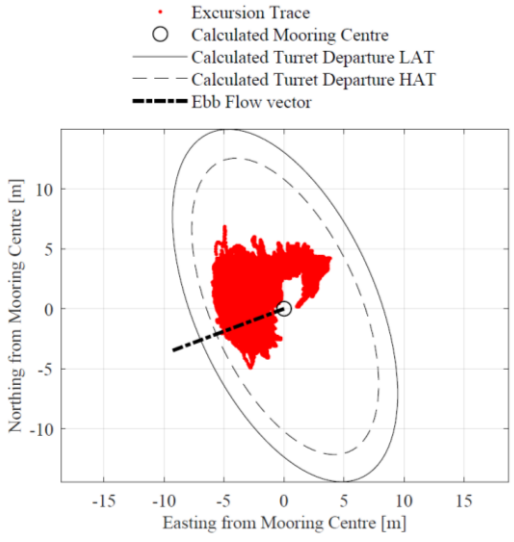

Figure 9: PLAT-I turret position with Parked turbines

The motion caused by the velocity can be seen in Figure 10 to follow the same pattern as that when the SDMs are up. The drogueing effect is increased, so at higher flow speeds the platform is more aligned with the flow, with less sideways excursion. When the velocity is higher, whether on the ebb or the flood, the motion is reduced, and the position becomes more concentrated. This is also seen in Figure 11 where position is stable over the mooring spread centre. The high concentration of positional data to the North East of the centre spread is the flood position with the offset applied, so is over the mooring centre. The concentration is lower on the ebb positional data as the platform moves slightly more due to the flow speed than with SDMs up.

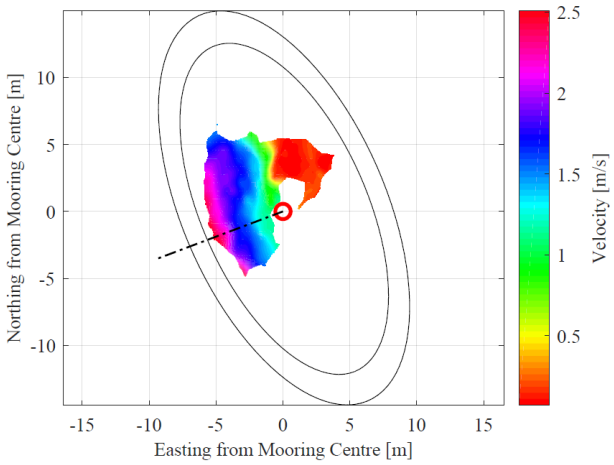

Figure 10: PLAT-I turret position with Parked turbines, with Velocity

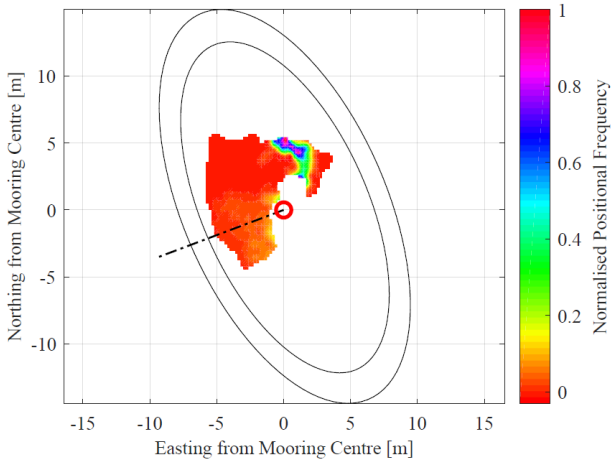

Figure 11: PLAT-I turret position with Parked turbines, with Occurrence

C. Operational

This result is even more pronounced when the turbines are generating, as they exert significant thrust, which pulls the platform into alignment with the flow. This can be seen in Figure 12 which shows excursion on the ebb only. The lateral motion is significantly reduced, and the position is always in a dropped back position (minimising the catenary effect). The platform moves further aft (SW) with increased flow, as seen in Figure 13, with the position in high flow and low depth (due to ebbing tide) close to the LAT excursion limit.

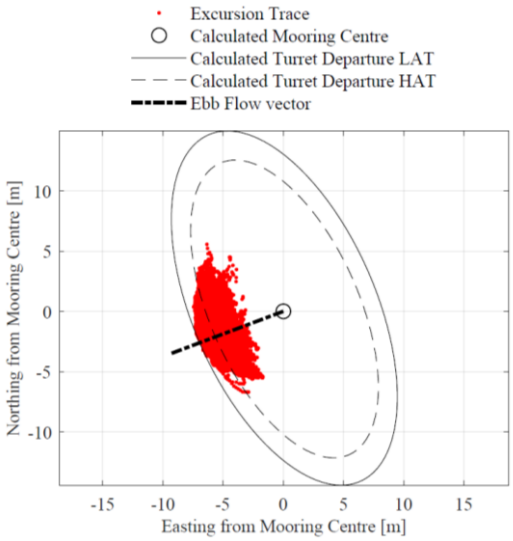

Figure 12: PLAT-I turret position with Operating turbines

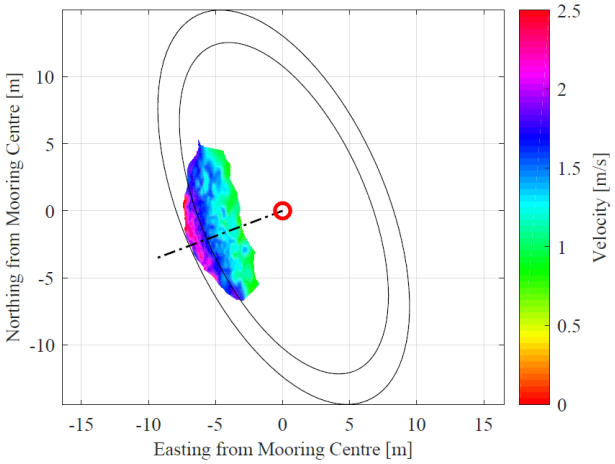

Figure 13: PLAT-I turret position with Operating turbines, with Velocity

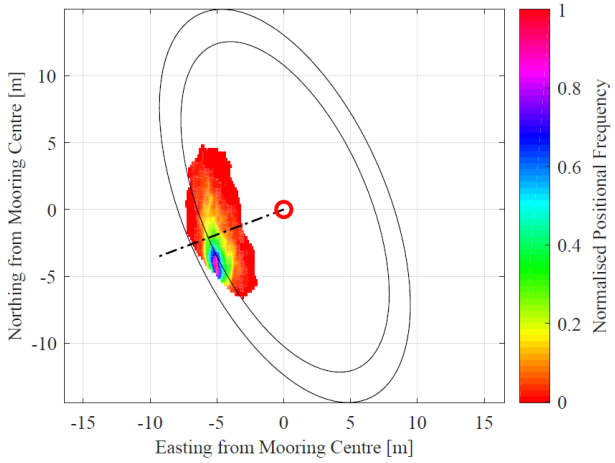

Figure 14: PLAT-I turret position with Operating turbines, with Occurrence

The frequency of occurrence, however, is not always directly in line with the ebb vector, shown in Figure 14. This is because there is stronger flow on the North side of the platform (which is particular to this site as discussed in Part 1), so the Port turbines exert more thrust, causing a load imbalance across the rotors. The mooring lines on the North side are also slightly longer causing the platform to translate to the South. The balance between rotational and translation effects can also be investigated further using rotational angle data. Despite this movement to one side of the ebb vector the position is very stable. This asymmetry would not occur in a more linear and less spatially varying site but is caused by the jet feature of the site.

The system can be seen to be stable and within the limits of excursion for all modes of operation. The lateral motion reduces with increased drag and thrust, and resistance to side motion, and the longitudinal motion (in line with velocity vector) increases with flow speed as the catenary effect is minimised.

VII. Mooring Load

Loads generated by the rotors, SDMs, hulls, and moorings are all translated into the mooring system and thus the load shackle. When the platform is orientated to the ebb tide the load shackle is situated on the upstream mooring line.

In order to compare the performance with predictions the mooring line load for the SDMs Up, Parked and Operating cases were assessed.

A. SDMs Up

The SDMs Up load is shown in against velocity. As shown in Part 1 there are differing numbers of data points in each bin; as per IEC TS-62600, any data sets with less than 30mins data have been denoted as Non-IEC in this analysis. The load measured is quite comparable to the prediction, though there is a slight difference. This is most likely caused by the lack of representation of some bodies in the engineering predictions, such as the load bank which dissipates the power to the water which also imparts a drag load, and the static pre-tension load of the mooring lines, as the bifurcated lines cannot be modelled accurately in the simulation software.

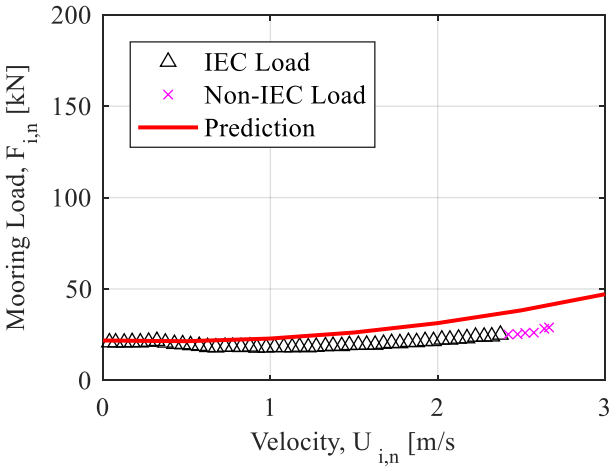

Figure 15: Mooring Load against Velocity for SDMs Up

The pre-tension in the mooring lines is a function of the platform position relative to the anchor points and is generated by the chain's catenary. The static trim is also affected by the centre of gravity. This changes with operational mode, as the turbine weight moves aft as the SDMs are raised; this is not however accounted for in the engineering predictions. For this reason, the mooring load is higher at low flow speeds where the system is trimmed further aft. As the platform levels with velocity the load reduces to a minimum at approximately 1m/s. Higher velocity then causes forward trim and higher drag, so the mooring line load increases again.

B. Parked

With parked turbines (Figure 16) the prediction is again comparable, with a slight offset from the prediction due to static pre-tension. There are less IEC compatible data points between 0.5m/s and 1m/s because during flood tide the flow speed rarely exceeds 0.5m/s, and on the ebb the slack water period is short with speed increasing to above 1m/s rapidly. This gives few data points in the range between these values. There are also fewer data points at high speeds due to the turbulent nature of the site, as shown in Part 1.

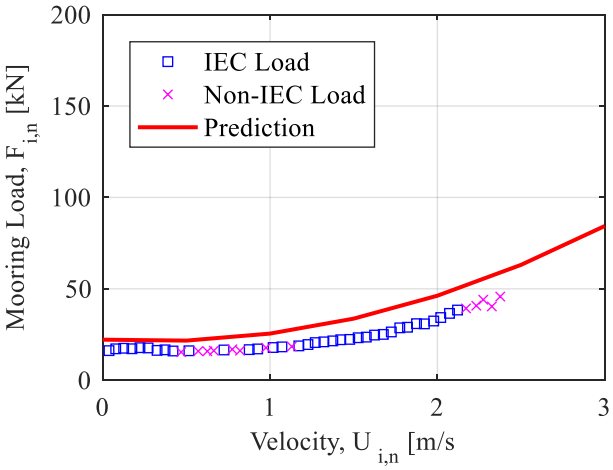

Figure 16: Mooring Load against Velocity for Parked Turbines

C. Operating

The static offset is also observed for the operating load (Figure 17). In these results all four turbines must be operating, which results in fewer data points with 30mins of data since the site has high spatial variation and turbulence.

The engineering prediction must be tailored to account for power and thus thrust variation between the rotors, caused by the spatially varying flow. To obtain the operating predictive load, the platform total power is obtained, then averaged across the four turbines. The respective thrust for this average power is then used in the numerical models to simulate the platform load (though the velocity will still be higher than the average across all the rotors since it is measured on the Port side of the platform). The platform must be treated as a whole rather than the turbines individually, as the load from all the turbines

translates through the system to the mooring lines. The measured load is comparable to the prediction but can be seen to be slightly lower than the predicted load. This will be further investigated in subsequent sections.

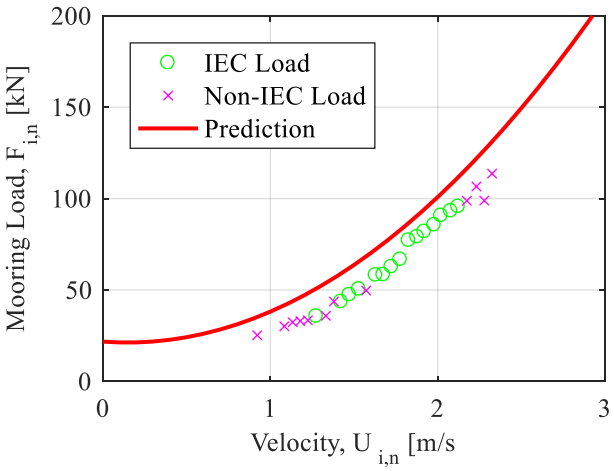

Figure 17: Mooring Load against Velocity for All Operating Turbines

D. Operational Mode Comparison

The mooring line load for each of the modes of operation were corrected by subtracting the minimum parked load (static pre-tension) from the field results and the predictive results. This removes discrepancy caused by the line tensions as simulated, due to limitations in the numerical model. The corrected loads are shown in . This shows the higher load at low flows for SDMs up due to the centre of gravity and thus pitch aft. It also shows the increase in load with velocity, and also with increased drag with SDMs down and then operational turbines thrust.

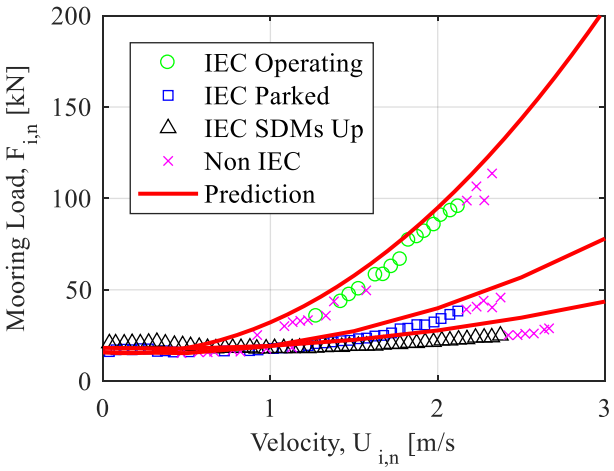

Figure 18: Mooring Load against Velocity for Parked Turbines

With the static pretension offset the predictive load is very comparable to the field load. There is still some difference between the field and predictive results, but it gives good confidence in the system performance.

Additionally, at future more linear and less turbulent sites, the discrepancy at higher velocities, seen here above 2m/s will not be seen, as there will be more data points and less turbulence and variation at high flow speeds. There will also be les variation across the rotors and the flow sped will be more representative of the flow across the whole platform.

VIII. SDM LOAD

The reaction load recorded at the SDM pin is derived from the forces acting on the SDM (Figure 19), which is predominantly caused by rotor thrust, but also the drag of the SDM and nacelle, the mass of the turbine, the mass of the rotors, and the reaction at the hinge. This can be resolved into thrust acting at the rotor axis, to give a thrust comparison with engineering predictions. The load, and dominant contributions, therefore changes for the different modes of operation:

- SDMs up – zero load on system
- SDMs only – load on system due to fit in brackets, and drag on the SDMs and nacelle only
- Parked – load on system due to fit in brackets, drag on the SDMs and nacelle, and drag due to the parked rotor
- Generating – load on system due to fit in brackets, drag on the SDMs and nacelle and, predominantly, rotor thrust.

Figure 19: Forces acting on SDMs (left) and photo of SDM (right)

A. Pull Tests

In order to calculate the thrust for a given reaction the components acting about the hinge can be resolved, but this could cause error due to inaccuracies in mass and buoyancy (magnitude and position). A pull test was performed at site with the SDMs in situ, to give a reaction-load-to-thrust-applied relationship. This was used to determine the thrust (and drag) acting at the nacelle for the field tests.

B. SDMs Only

There are no results for SDMs Up as there is no thrust acting on the pins for this condition.

The reaction recorded when the SDMs are lowered without the SITs attached can theoretically be resolved to give the drag of the system. However, in order for the load pin to read a value then the force balance of the system must be overcome. Since the drag of the SDM is so low then the load pin only reads a static value. The drag of the system cannot therefore be isolated.

C. Parked

The reaction loads recorded when the SDMs and SITs are lowered but in Parked mode were also recorded. The reaction load recorded was resolved using the relationship determined from the pull test to the force acting at the nacelle axis. The resulting loads are shown in Figure 20. The null value calculated from flow speeds below 0.25m/s (where the force balance is not overcome) is between 2.3 and 3.3kN depending on the SDM pin, so results below this threshold +0.1kN are removed. The variation between the SDMs can be seen in alignment of velocity variation, i.e. SIT1 experiences most flow speed and therefore thrust, whereas SIT4 experiences the least.

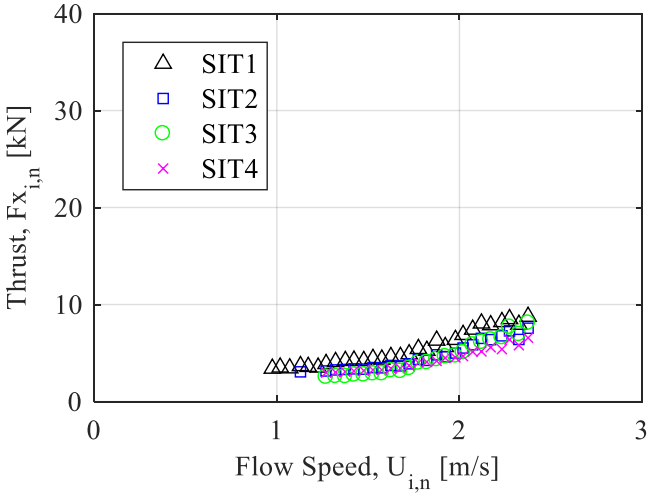

Figure 20: Rotor Drag against Velocity for all Parked turbines

Figure 21 shows the force measured acting at the nacelle for SIT2 (since this is directly downstream from the velocity measurement), with the prediction from BEM models, as discussed in Part 1. The results are higher than the prediction, which is expected since the results include SDM and nacelle drag. This is expected to be low and circa 2kN but cannot be definitively resolved. There may also be some discrepancy due to highly fluctuating inflow and additional side loading due to eddies. When comparing the results for SIT2, which is closest to the velocity measurement, the measured drag is 1 and 2kN, approximately the predicted drag value. This gives good confidence in the readings from the SDM pins for SIT2.

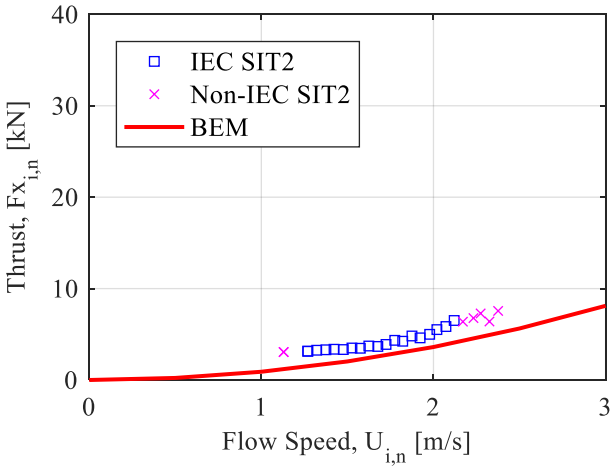

Figure 21: Rotor Drag against Velocity for Parked SIT2

D. Operating

The reaction was recorded when the turbines were in Operating mode and above the Parked null value (as there is no slack water result for Operating turbines since they cut in at higher flow speeds, and the Parked configuration is the same as the operating). The operating thrust of each rotor including SDM and nacelle drag are shown in Figure 22.

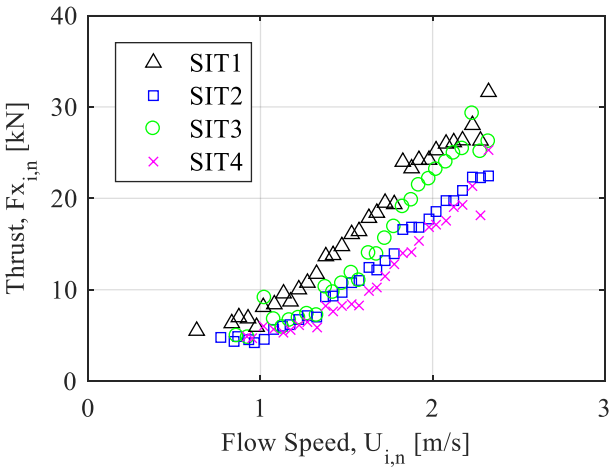

Figure 22: Rotor Thrust against Velocity for Operating turbines

The variation between the rotors has changed from the previous distribution, where thrust varied with the expected velocity variation (strong flow at SIT1 through to weak flow at SIT4). Here, however, SITs 1 and 3 create more thrust than SITs 2 and 4; this thrust variation is currently under investigation. Possible causes are most likely attributable to the rotational direction, as the SITs are paired CW and CCW, as shown in Part 1.

The performance comparison for SIT2, closest to the velocity measurement, shows that the thrust curve is close to the prediction, though it should produce higher thrusts due to the SDM and nacelle drag which cannot be isolated.

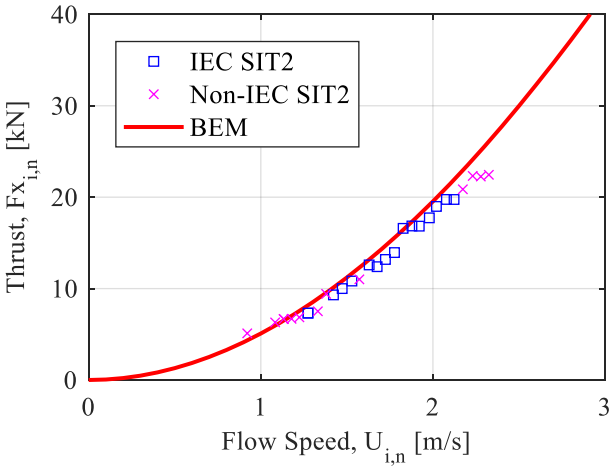

Figure 23: Rotor Thrust against Velocity for Operating SIT2

If the thrust results are assessed independently of the velocity we can compare the power-thrust curves, as shown below in Figure 24. This shows that SITs 1and 3 produce more thrust for power generated than SITs 2 and 4. This will be further investigated during SATs.

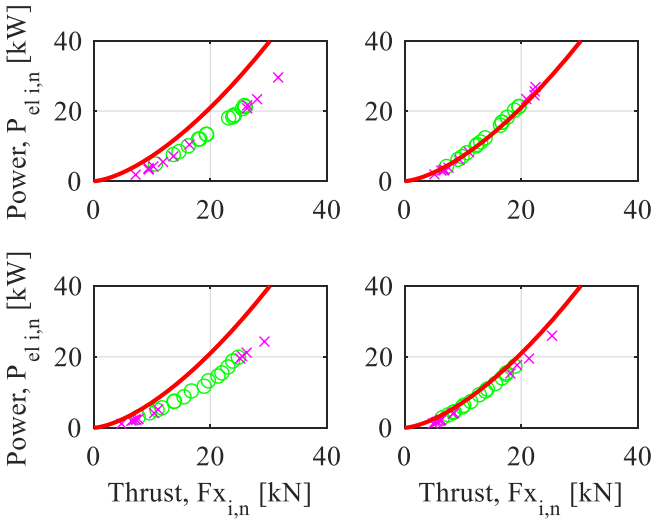

Figure 24: Rotor Thrust against Produced for SIT1 (top left), SIT2 (top right) SIT3 (bottom left) and SIT4 (bottom right)

The measured mooring load was also lower than that expected, as previously shown, and so this difference is further investigated.

The mooring line load against platform (all four turbines) power shows that the curve for the field results and the prediction are highly comparable (Figure 25); however, the total thrust is consistently higher than the prediction against mooring load. This may be due to the drag of the SDMs and nacelle but does not account for the handedness of the thrust.

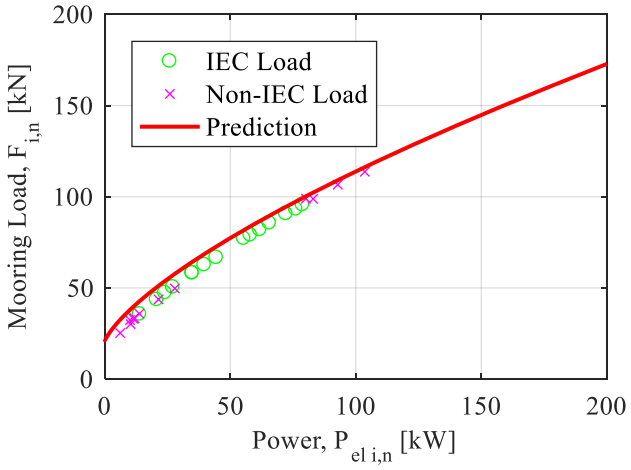

Figure 25: Platform Power against Mooring Load

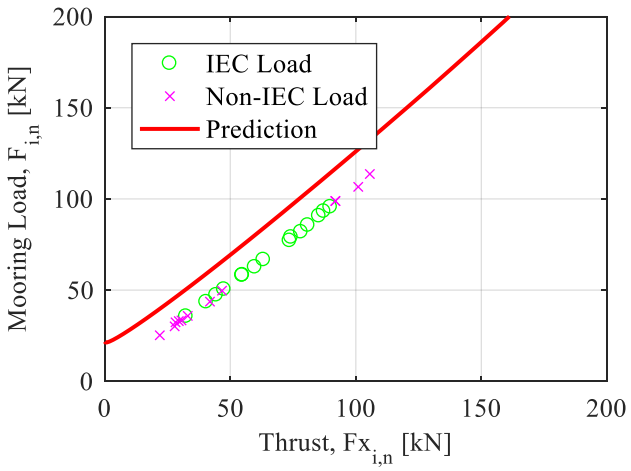

Figure 26: Platform Thrust against Mooring Load

As an alternative assessment, the mooring line load for the Parked condition was subtracted from the Operational values for each flow speed bin, so that the difference in mooring tension between parked and operational was obtained from the measured values. This was resolved into the x-direction using the mooring line angle to give an axial load difference for the mooring line. The total (sum) measured drag load for the Parked condition was subtracted from the total thrust and drag load for the Operating cases, to give the difference in thrust as recorded by the SDM load pins. The results for these two load differences are shown in Figure 27.

The resolved thrust as calculated from the mooring load is comparable to the measured thrusts for the platform, but there is still a difference. This requires further internal investigation.

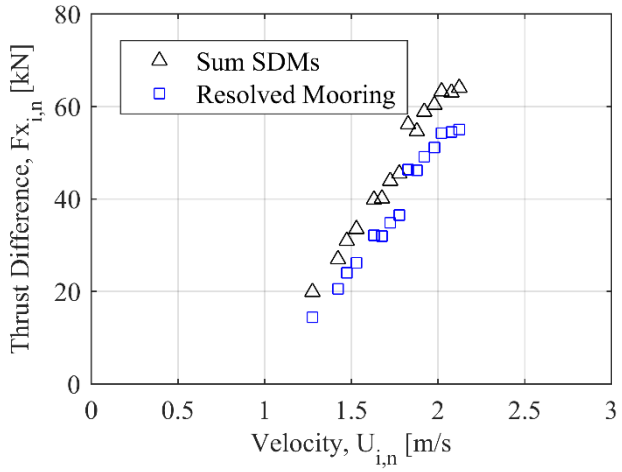

Figure 27: Comparison of Measured Thrust and X-Component of Mooring Load for All Turbines Operating

E. Operational Mode Comparison

Even though there is some difference between the load pins the effect of each operational mode can be assessed. Since SIT2 is closest to the velocity sensor this will be compared for each mode (Figure 28). The results show that the load increases with the addition of turbine operation as might be expected.

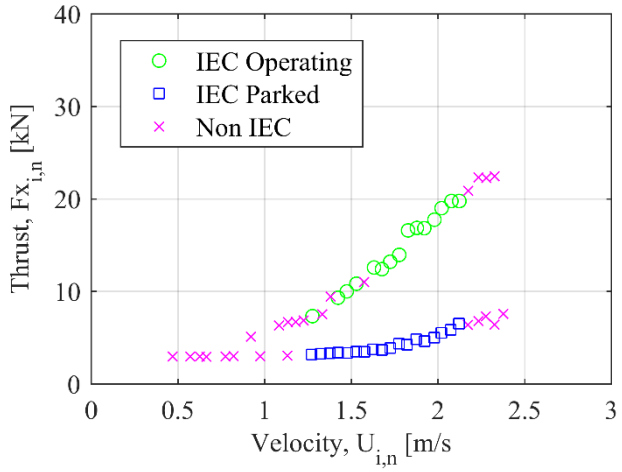

Figure 28: Thrust against Velocity for all Platform Modes

IX. Conclusions

1. Motion, SDM load and mooring load are all directly related to velocity and thus drag. They are therefore also affected by mode of operation, due to the change in wetted area and thrust loading.
2. Position and mooring line loads are as expected from engineering design work, using numerical models, with some allowance for error due to thrust and pre-tension discrepancies.
3. However, SDM loads are higher than expected for Parked turbines, as they include SDM and nacelle drag, and lower than expected for operating turbines.
4. Differences between measured and predicted thrust loads from the turbines, and the isolation of drag, will be further investigated.

Acknowledgements

This work has been supported by the EPSRC funded SURFTEC (SUrvivability and Reliability of Floating Tidal Energy Converters) project (EP/N02057X/1).

References

[1] J. McDowell, P. Jeffcoate, M. Khorasanchi, L. Johanning and T. Bruce, "First Steps towards a Multi-Parameter Optimisation Toll for Floating Tidal Platforms – Assessment of an LCOE-Based Site Selection Methodology," in *Proc. EWTEC'17*, 2017

[2] European Marine Energy Centre. Available at: www.emec.org.uk

[3] Scotrenewables.SR2000. Available at: http://www.scotrenewables.com/technology-development/sr2000

[4] Sustainable Marine Energy. Available at: www.sustainablemarine.com

[5] SCHOTTEL Hydro. Available at: https://www.schottel.de/schottel-hydro/

[6] N. Cresswell, J. Hayman, A. Kyte, A. Hunt, P. Jeffcoate, "Anchor Installation for the Taut Moored Tidal Platform PLAT-O" in *Proc. AWTEC'16*, 2016.

[7] R. Starzmann, I. Goebel, P. Jeffcoate, (2018) "Field Performance Testing of a Floating Tidal Energy Platform – Part 1: Power Performance" in *Proc. AWTEC'18*, 2018.